The effect of Ru-site dopants on the magnetic properties of $CaRuO_3$

2001 J. Phys.: Condens. Matter 13 8347

(http://iopscience.iop.org/0953-8984/13/36/309)

INSTITUTE OF PHYSICS PUBLISHING JOURNAL OF PHYSICS: CONDENSED MATTER

J. Phys.: Condens. Matter **13** (2001) 8347–8361 PII: S0953-8984(01)24244-1

The effect of Ru-site dopants on the magnetic properties of $CaRuO_3$

T He[1] **and R J Cava**

Department of Chemistry and Princeton Materials Institute, Princeton University, Princeton, NJ 08540, USA

E-mail: taohe@princeton.edu

Received 25 April 2001, in final form 17 May 2001
Published 23 August 2001
Online at stacks.iop.org/JPhysCM/13/8347

Abstract

The effects of Ru-site metal dopants on the low-temperature magnetization of $CaRuO_3$ are reported. Dopants of two types are tested: those with closed d shells in their expected oxidation state (Al^{3+}, Zn^{2+}, Ti^{4+}, V^{5+} and Pt^{2+}), and those with unpaired d electrons (Mn^{4+}, Fe^{3+}, Co^{2+}, Ni^{2+} and Cu^{2+}) in their expected oxidation state. The results are consistent with the recent proposal that $CaRuO_3$ is not a classical antiferromagnet, but rather is poised at a critical point between ferromagnetic and paramagnetic ground states. Ti, Fe, Mn and Ni doping result in ferromagnetic behaviour.

1. Introduction

The ruthenate perovskites have been of interest in the study of the magnetism of complex systems [1–9]. The compounds evolve from ferromagnetism to superconductivity between three-dimensional (3D) $SrRuO_3$ and two-dimensional (2D) Sr_2RuO_4 [1–4], and from ferromagnetism to paramagnetism between $SrRuO_3$ and $CaRuO_3$ in 3D materials [10–13]. The understanding of the $CaRuO_3$ perovskite, long described as a paramagnetic material with antiferromagnetic spin interactions, therefore establishing a baseline for 'normal' magnetic behaviour in this system, has recently been called into question. Based on NMR studies of the magnetic interactions, a new context for understanding $CaRuO_3$ has been proposed, in which $CaRuO_3$ is considered to be a nearly ferromagnetic metal, rather than a classical Curie–Weiss antiferromagnet [14–17]. We have recently shown that a small amount of disorder introduced into $CaRuO_3$ by partial substitution of Ru by non-magnetic, isovalent Ti^{4+} induces clear ferromagnetic behaviour at low temperatures [18]. This confirms the proposal that $CaRuO_3$ itself is poised at the edge of ferromagnetic behaviour, as a small disruption of the Ru sublattice changes the properties dramatically. Non-Fermi-liquid behaviour has also been observed in

[1] Author to whom correspondence should be addressed.

the transport properties of $CaRuO_3$ [19], further establishing the unusual character of this material.

Here we present the results of more extensive studies of the effects of Ru-site dopants on the magnetic properties of $CaRuO_3$. These studies were performed in part to determine whether the effects of Ti doping are unique, and in part to see how the system evolves on disruption of the Ru sublattice by different types of magnetic and non-magnetic atom. The dopant metals are selected to span the 3d transition metal series, and thus electron count, with additional atoms such as Al and Pt. These are tested as Al and Pt are expected to be common impurities incorporated by crucible reaction during synthesis of $CaRuO_3$. Rh and Sn doping of $CaRuO_3$ has been previously reported [20, 21], and is not studied further here. A recent report on the magnetic and transport properties of $CaMn_{1-x}Ru_xO_3$ from the viewpoint of colossal magnetoresistance [22] is fully consistent with our results. We find that some dopants have significant effects on the magnetism of $CaRuO_3$ while others have only modest effects. Pt, V, Co and Cu, for example, have little effect on the Curie–Weiss temperature and the hysteresis loops at low temperatures, if any are displayed at all, are very small. Some 3d transition metals, especially Fe and Mn, have large effects on the magnetic properties. They shift the Curie–Weiss temperature to much less negative (or in some cases positive) values and yield large low-temperature hysteresis loops. For these substitutions, the magnetization is greatly enhanced at high fields at low temperatures indicating strong ferromagnetism. Low-field magnetization measurements show that the temperature at which ferromagnetism turns on is only dependent on the dopant atom, and not on dopant concentration under our conditions of synthesis.

2. Experiment

Samples of $CaRu_{1-x}M_xO_3$ ($x = 0.05$, and $x = 0.25$, in general) for M = Al, Zn, Pt and the 3d transition metals from Ti to Cu were prepared by conventional solid-state reaction. Starting materials were $CaCO_3$ (99.8% Mallinckrodt), dried RuO_2 (99.95% Cerac) and the corresponding metal oxides: Al_2O_3, ZnO, PtO_2, TiO_2, V_2O_5, Cr_2O_3, MnO_2, Fe_2O_3, Co_3O_4, NiO and CuO. For some substitutions, M = Fe and M = Mn, additional compositions were synthesized. For all dopants except Pt, the starting materials were mixed in stoichiometric proportion and heated in dense Al_2O_3 crucibles at 1000 °C in air for 2 days with intermediate grindings. The powders were then pressed into pellets and heated in dense Al_2O_3 boats at 1250 °C in air for 1 day. $CaRu_{0.99}Pt_{0.01}O_3$ was made by mixing starting materials in stoichiometric proportion and heating in a dense Al_2O_3 crucible at 800 °C in O_2 for 2 days. The sample was then annealed at 580 °C in O_2 for 40 hours. All samples were investigated by x-ray powder diffraction with Cu Kα radiation at room temperature.

The magnetic properties were studied in a Quantum Design PPMS system, which uses the extraction method for measuring magnetization. For all samples, the magnetization was measured in the temperature range 5–300 K in an applied DC field of 10,000 Oe on field cooling. The Mn and Fe doped samples were also studied in an applied DC field of 1000 Oe on field cooling. All the magnetic hysteresis loops were taken at 5 K. The highest magnetic field applied ranged from 20,000 to 90,000 Oe depending on the dopant.

3. Results and discussion

The purity of the $CaRu_{1-x}M_xO_3$ samples was checked by x-ray powder diffraction. All the successfully doped materials have the $GdFeO_3$-type orthorhombic perovskite structure. At

5% doping, all the materials are pure phases, except for the dopants Pt and Cr. The highest achievable doping level for Pt was 1% and no single-phase material was found for Cr doping, even at the 1% level. For some of the transition metals, single-phase perovskites were also obtained at the 25% doping level. These metals were Ti, Mn, Fe, Co and Zn. For Ni, which had a large effect on the magnetic properties of $CaRuO_3$ at the 5% substitution level, 10% substitution was found to yield multiple phase material. For Mn and Fe, where the magnetic properties were strongly affected, perovskites were made for higher amounts of substitution to follow the development of the properties. Under our conditions of synthesis, substitution at the 33% Fe and 75% Mn level was possible, retaining single-phase structure.

The 5% doping samples will be considered as two general groups, depending on whether the dopant is expected to have a closed or open d shell for the expected oxidation state under the conditions of synthesis. The first group includes Al^{3+}, Zn^{3+}, Ti^{4+}, V^{5+} and Pt^{2+}(1%), with d^0 or d^{10} configurations. The second group includes Mn^{4+}, Fe^{4+}, Co^{2+}, Ni^{2+} and Cu^{2+} with various numbers of d electrons. For this latter group, preliminary oxidation states are assigned by analogy with results on the closely related hexagonal compounds $Ba_3Ru_2MO_9$ [23–25].

The temperature dependence of M/H for the first group of samples is shown in the upper panel of figure 1. These data were taken in an applied DC field of 10,000 Oe on field cooling. The 1% Pt doping and 5% V doping do not have much effect on the magnetic properties of $CaRuO_3$. The 5% Al, Zn and Ti doping has a greater effect as seen in the higher M/H values at 5 K. The lower panel of figure 1 shows the temperature dependence of H/M for the first group of samples. All samples, including $CaRuO_3$ itself, show an S-shaped downward trend below 50 K, as observed in $CaRu_{1-x}Ti_xO_3$ [18]. For this group of samples, Al doping has the largest effect on magnetization. This is of particular interest as Al_2O_3 crucibles are commonly employed in ruthenate synthesis. Though little Al accommodation is expected under normal conditions of synthesis, very small amounts of Al impurities have, for example, been shown to significantly affect the superconductivity in Sr_2RuO_4 [26].

The behaviour of M/H and H/M as a function of temperature for the second group of samples is shown in figure 2. The S-shaped downward trend in H/M is again observed for these substitutions. The 5% Co, Cu and Mn-doped samples display magnetization comparable to that seen in the first group. The 5% Mn doping, however, shows an enhancement in M/H in the intermediate temperature range. The 5% Fe and Ni substitutions have a much greater effect, as seen in the fivefold higher M/H values at 5 K. The data for these two substitutions are shown in the inset of the upper panel of figure 2: much sharper decreases in H/M are seen below 100 K.

For all 5% doped samples, the high temperature data can be described well by fitting to the Curie–Weiss law. The effective magnetic moment per formula unit, μ_{eff}, and the Curie–Weiss temperature, θ_{CW}, both derived by fitting the data between 175 and 300 K, are shown as a function of the dopant in the upper and middle panels of figure 3. A small temperature-independent term, χ_0, was included in the fits, determined to a precision of $\pm 5 \times 10^{-5}$ emu/mol formula unit. The dopants span the 3d series from $3d^24s^2$ (Ti^0) to $3d^{10}4s^2$ (Zn^0). The effective magnetic moment per mole formula unit, μ_{eff}, falls between 2.8 μ_{B} fu^{-1} and 3.2 μ_{B} fu^{-1}. The dopants with closed shells, Ti^{4+}, V^{5+}, Zn^{2+} and Al^{3+}, might be expected to decrease μ_{eff} to approximately $0.95 \times 3.1 = 2.95$ μ_{B} fu^{-1} by simple dilution if the Ru moment is unchanged (considering the formula $CaRu_{0.95}M_{0.05}O_3$). Only for Fe^{3+} and Co^{2+} doping μ_{eff} is not decreased. The increase may be due to both, the moments of the dopants, and the possible inducing of Ru^{5+} ($S = 3/2$), which has a higher moment than Ru^{4+} ($S = 1$). The low μ_{eff} values which result from Mn^{4+} ($S = 3/2$) and Ni^{2+} ($S = 1$) doping are somewhat unexpected as these ions have moments higher than or similar

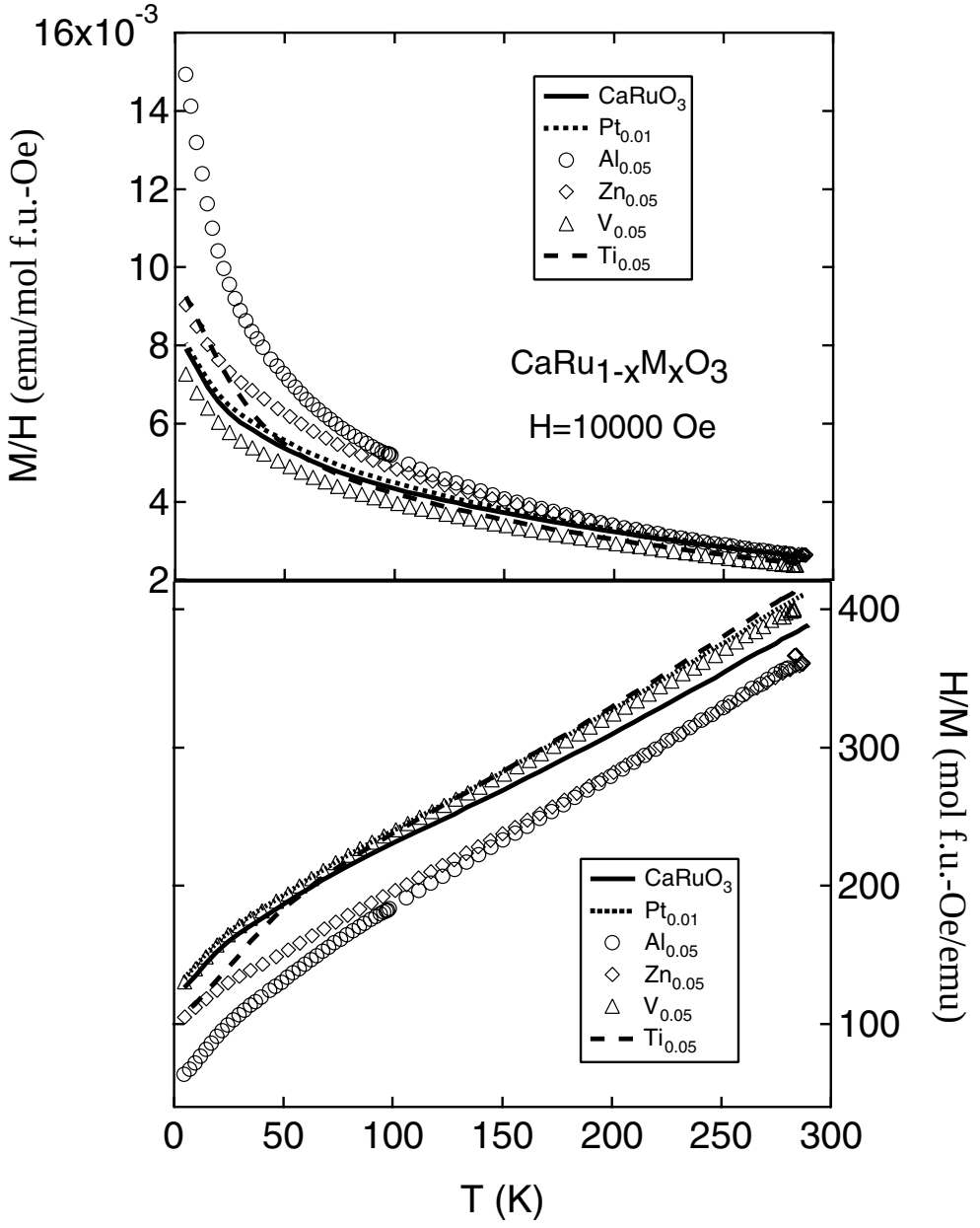

Figure 1. Temperature dependence of M/H (upper panel) and H/M (lower panel) measured at 10,000 Oe on field cooling for $CaRu_{0.95}M_{0.05}O_3$ (M = Pt, Al, Zn, V and Ti).

to Ru^{4+}, and in the Ni case would induce the presence of significant quantities of Ru^{5+}. Even if the Ni were to be accommodated as spin zero Ni^{3+}, Ru^{5+} is still expected to form. The real picture is certainly not so simple as adding all the moments together in a localized type model such as described here because the magnetism in the perovskite ruthenates is more

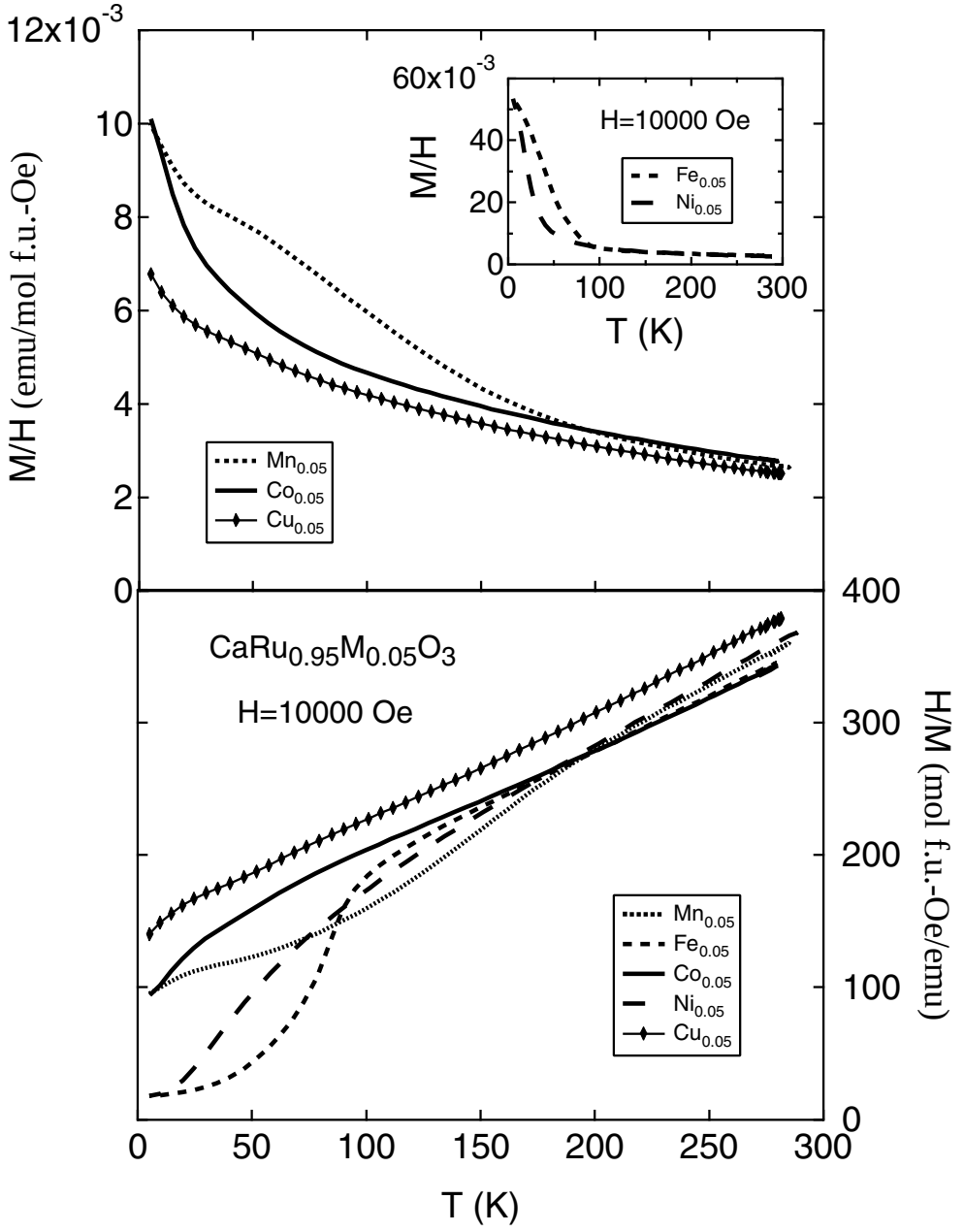

Figure 2. Temperature dependence of M/H (upper panel) and H/M (lower panel) measured at 10,000 Oe on field cooling for $CaRu_{0.95}M_{0.05}O_3$ (M = Mn, Fe, Co, Ni and Cu).

appropriately described in the band picture rather than in the localized spin picture applicable to insulators. However, the local moment picture can serve as a baseline for more detailed investigation of the effects of specific dopants.

The middle panel of figure 3 shows θ_{CW} for the series. With the exceptions of V, Co and Cu doping, all other dopants lead to a much less negative θ_{CW} than that found for $CaRuO_3$,

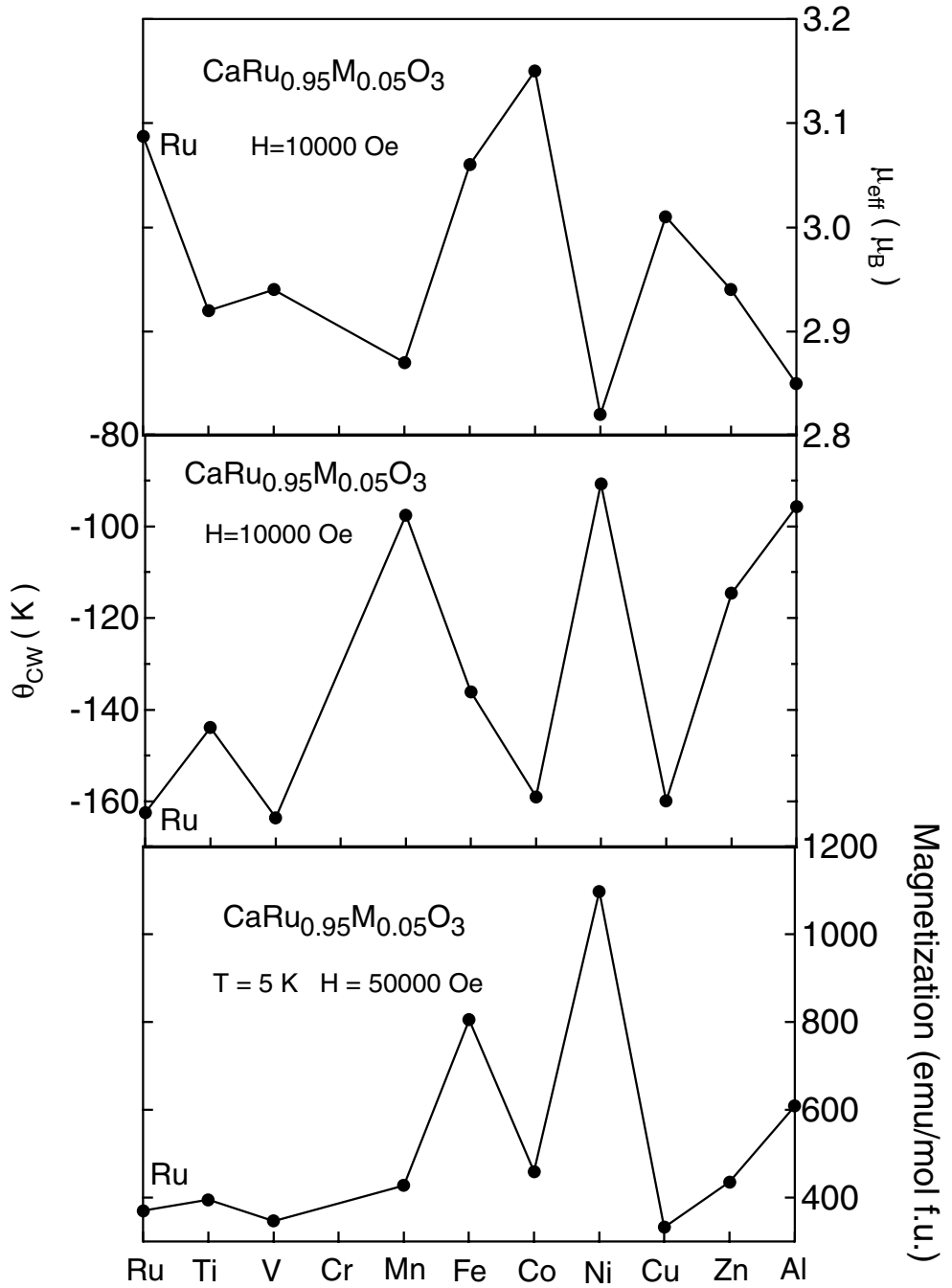

Figure 3. The effective magnetic moment per mole formula unit (upper panel), the Curie–Weiss temperature (middle panel) and the magnetization at 5 K in an applied field of 50,000 Oe (lower panel) for $CaRu_{0.95}M_{0.05}O_3$. Solid lines are guides to the eye.

indicating a general trend towards increased ferromagnetism on any disruption of the Ru–O network. Mn, Ni and Al doping are especially effective at changing θ_{CW}. The results of the

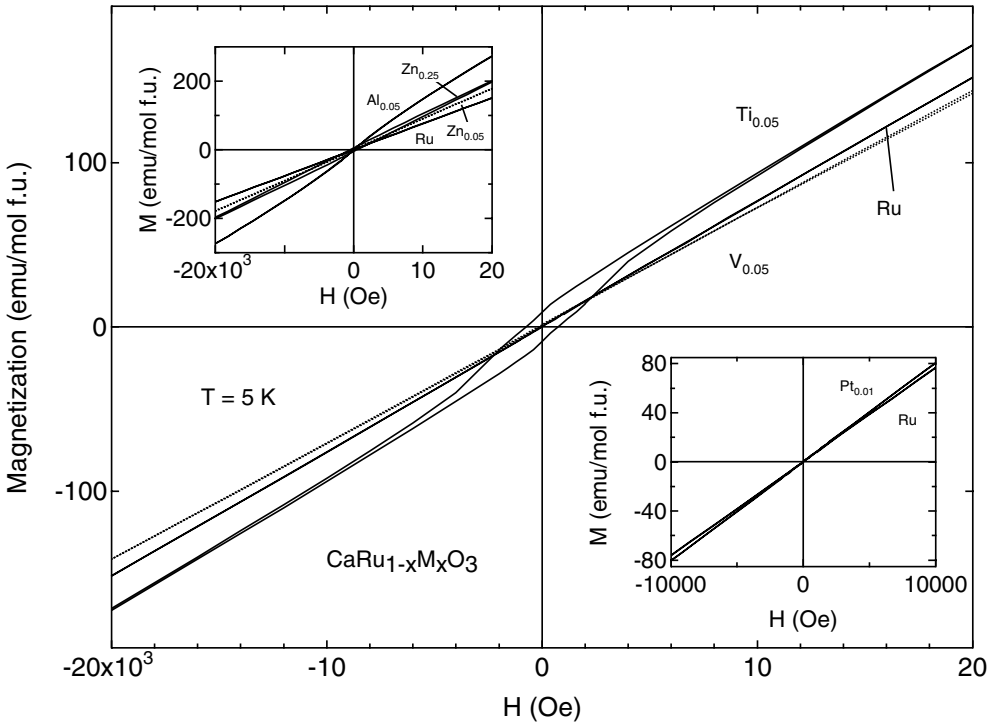

Figure 4. Magnetic hysteresis loops for $CaRu_{0.95}M_{0.05}O_3$ (M = Pt, Al, Zn, V and Ti) at 5 K.

doping experiments reinforce the questions about the meaning of θ_{CW} in $CaRuO_3$. In earlier discussions, the large negative θ was taken to indicate the dominance of antiferromagnetic interactions [1]. Recently however, an alternative picture has been proposed for $CaRuO_3$ in which the dominant interactions are ferromagnetic [14–17]. In this picture, the sign and magnitude of θ_{CW} can be considered as an order parameter for measuring the change from a conventional band ferromagnet such as is seen in $SrRuO_3$ to an exotic magnetic state such as is displayed in $CaRuO_3$. Thus we interpret the data in the middle of figure 2 as showing which dopants most effectively disrupt the unusual magnetic state of $CaRuO_3$ and drive the system towards ferromagnetism. Those which most change the θ_{CW} in a positive direction have been the most effective at suppressing the unconventional behaviour and stabilizing the 'expected' ferromagnetic behaviour of $CaRuO_3$.

The S-shaped downward trend in M/H and the less negative θ_{CW} both suggest that some of the dopants may give rise to ferromagnetism in $CaRuO_3$. Magnetization field measurements were therefore performed to test for ferromagnetism. Figures 4 and 5 show the magnetic hysteresis loops measured for all the samples at 5 K. One per cent Pt^{2+} doping is shown in the lower-right inset of figure 4. The effect of Pt is small and is seen only as a slight increase in the *M–H* slope compared to $CaRuO_3$. The magnetization data for the 5 and 25% Zn^{2+} doping and the 5% Al^{3+} doping are shown in the upper-left inset of figure 4. In an expanded scale, hysteresis loops are observed for all three samples, with a very small one for 5% Zn^{2+} doping. Obviously, Al^{3+} is more effective than Zn^{2+} in inducing ferromagnetism in $CaRuO_3$, but neither is as active as Ti^{4+}, which exhibits a rather large loop at 5 K. The 5% V^{5+} doping has little effect, and, in contrast to 1% Pt^{2+} doping, the *M–H* slope decreases. The five dopant atoms shown in figure 4 are all expected to have closed d shells in $CaRuO_3$

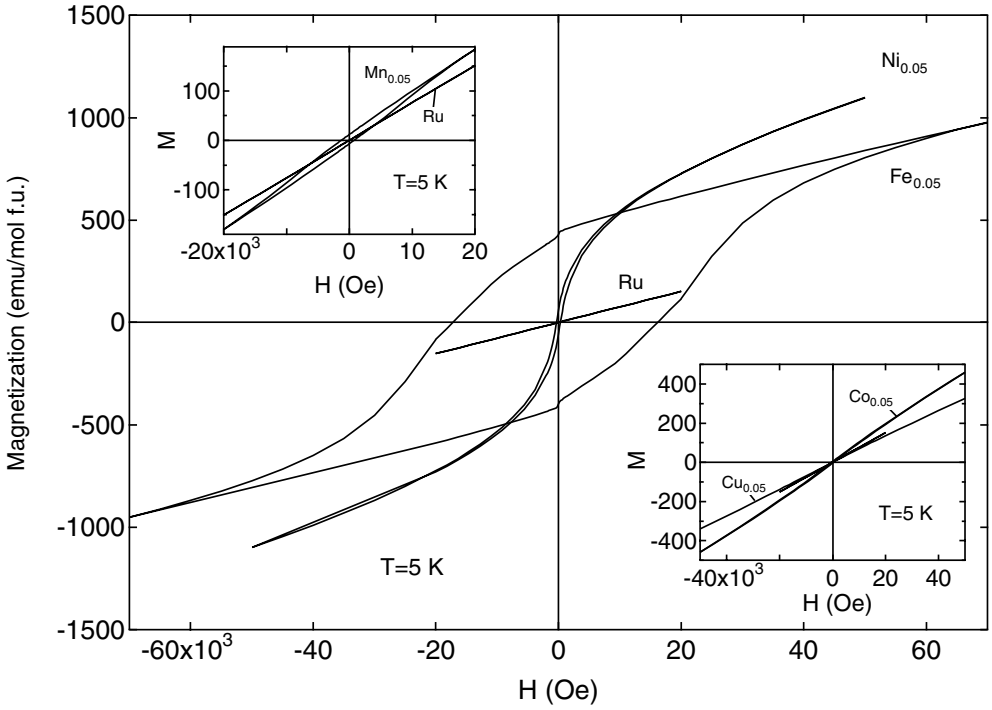

Figure 5. Magnetic hysteresis loops for $CaRu_{0.95}M_{0.05}O_3$ (M = Mn, Fe, Co, Ni and Cu) at 5 K.

and themselves would not be expected to contribute to magnetism. The effects observed may then be considered to be due to the degrees to which the different dopants disrupt the Ru^{4+}–O lattice of $CaRuO_3$. They do so by introducing electronic disorder, size disorder or changes in electron count, or a combination of these effects.

Figure 5 shows the magnetic hysteresis loops for the five 5% dopants expected to have unpaired d electrons on doping into $CaRuO_3$. The most extraordinary features are found for the Fe^{3+} and Ni^{2+} doping. Fe^{3+} yields a large, open hysteresis loop at low temperature with relatively large remanent magnetization and coercive field. Ni^{2+} doping, on the other hand, yields a large, narrow hysteresis loop with low remanent magnetization and low coercive field. The upper-left inset of figure 5 shows the magnetic hysteresis loop for Mn^{4+} doping, and the lower-right inset shows those for Co^{2+} and Cu^{2+} doping. Co^{2+} has an effect similar to Zn^{2+} (figure 4). Cu^{2+} has a similar effect to V^{5+}, which has a lower *M–H* slope than does $CaRuO_3$.

To summarize the effectiveness of the various dopants across the 3d series in inducing ferromagnetic behaviour in $CaRuO_3$, the magnetization at 50,000 Oe and 5 K is chosen for comparison purposes. This field is above that where the hysteresis loops are closed, if present, for all dopants. This comparison of the magnetizations is shown in the lower panel of figure 3. The low temperature magnetization shows a different trend from that of μ_{eff}. Two peaks are observed: one at 5% Fe^{3+} doping and another at 5% Ni^{2+} doping. The non-monotonic behaviour of all these quantities, θ_{CW}, μ_{eff} and M, across the 3d series indicates that the effects of doping cannot simply be an electron count effect in a band magnet: the observed behaviour cannot simply be the effect of adding different numbers of electrons into a broad band magnet in a systematic way as one traverses the 3d series. Rather, the electrons and their associated moments must be at least in part localized on the dopant ions and the changes the dopants induce in the surrounding Ru–O lattice must also be at least partially localized. Different dopants are expected to display different degrees of localized behaviour. This gives

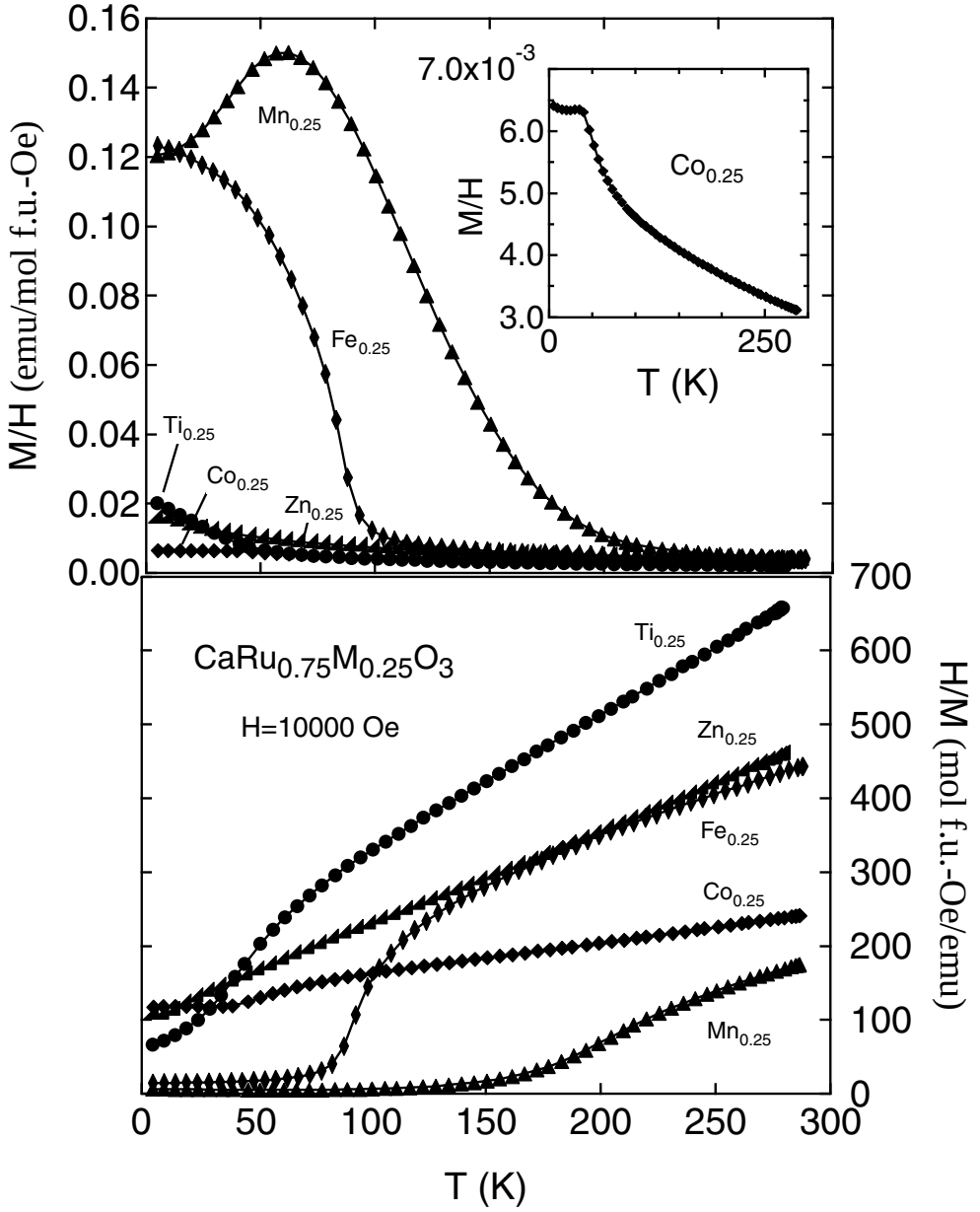

Figure 6. Temperature dependence of M/H (upper panel) and H/M (lower panel) measured at 10,000 Oe on field cooling for $CaRu_{0.75}M_{0.25}O_3$ (M = Ti, Mn, Fe, Co and Zn). Inset in the upper panel: temperature dependence of M/H for $CaRu_{0.75}Co_{0.25}O_3$.

rise to what is called an 'inhomogeneous' magnetic system in solid solution magnetic phases [22]. Distributions of dopant ions or clusters yield small-scale regions with different magnetic properties within the same phase.

To see how the magnetic properties of $CaRuO_3$ evolve on introducing a greater degree of substitution on the B-sites, a second set of materials, $CaRu_{1-x}M_xO_3$ with $x = 0.25$, was synthesized. Only Ti^{4+}, Mn^{4+}, Fe^{3+}, Co^{2+} and Zn^{2+} doping yielded pure perovskite

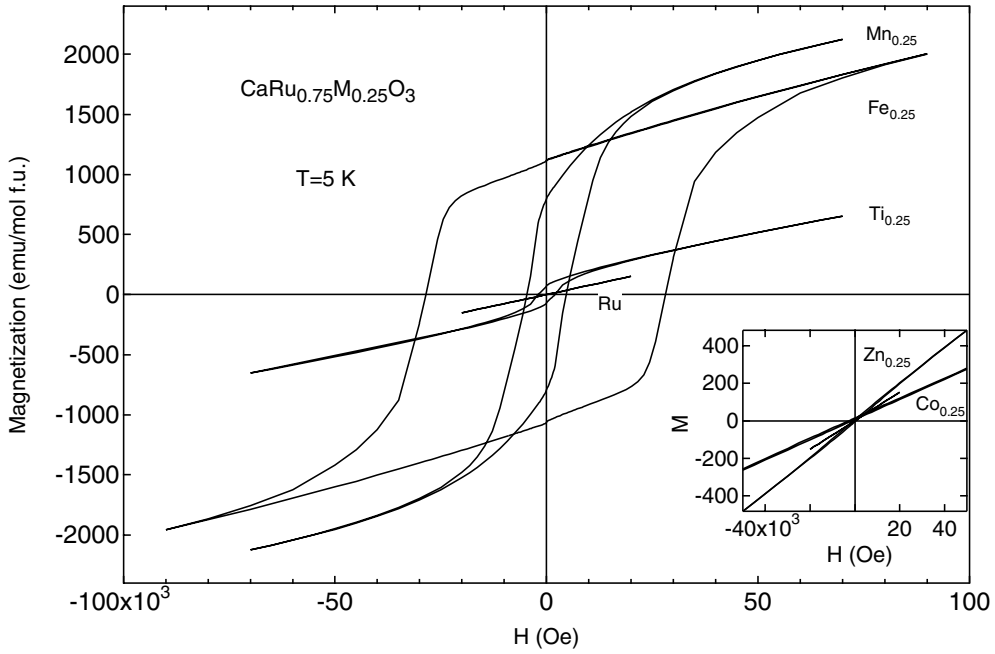

Figure 7. Magnetic hysteresis loops for $CaRu_{0.75}M_{0.25}O_3$ (M = Ti, Mn, Fe, Co and Zn) at 5 K.

materials at this level of substitution. The temperature dependence of M/H and H/M for these single-phase perovskites is shown in figure 6. The 25% Fe^{3+} and 25% Mn^{4+} doping shows the magnetization characteristics of a ferromagnet. The 25% Mn^{4+} doped material has a positive θ_{CW} but that for Fe^{3+} remains negative. The fact that the broad peaks seen in $M/H(T)$ are due to ferromagnetism in these two materials is confirmed by the presence of low temperature hysteresis loops. The 25% Co^{2+} doped perovskite, which is shown separately in the inset of the upper panel in figure 6, has a feature in $M/H(T)$ below 50 K which is more consistent with spin-glass behaviour than ferromagnetism. The low temperature M/H for the 25% Co^{2+} doped perovskite is much lower than that of the other dopants. In the lower panel of figure 6, $H/M(T)$, only the data for Ti^{4+}, Co^{2+} and Zn^{2+} doping can be described by fitting to the Curie–Weiss law in the highest temperatures of the measurement. The Mn and Fe doped materials display considerable curvature in the plots up to 290 K due to the presence of ferromagnetic fluctuations at high temperatures. θ_{CW} cannot be determined for these materials, but Mn^{4+} doping clearly yields a material with a positive θ_{CW}. Interestingly, Co^{2+} doping appears to result in a much more negative θ_{CW} than is found for $CaRuO_3$.

The magnetic hysteresis loops measured for all the 25% substituted samples at 5 K are shown in figure 7. The Fe^{3+} substitution shows a large, square hysteresis loop, similar to what was seen for the lower Fe doping level. Mn^{4+} doping yields a much narrower loop, though the saturation magnetizations are similar. Comparatively, the Ti^{4+} doping results in a material with a much lower magnetization at high fields but also a significant hysteresis loop. Co^{2+} and Zn^{2+} doping yield barely detectable or undetectable loops at the same level of sensitivity and are shown in the inset. All the dopants that have much less negative θ_{CW} values than $CaRuO_3$ show obvious hysteresis loops. For those dopants whose θ_{CW} values are similar to that of $CaRuO_3$, or even more negative (like 25% Co^{2+} doping), hysteresis loops are either

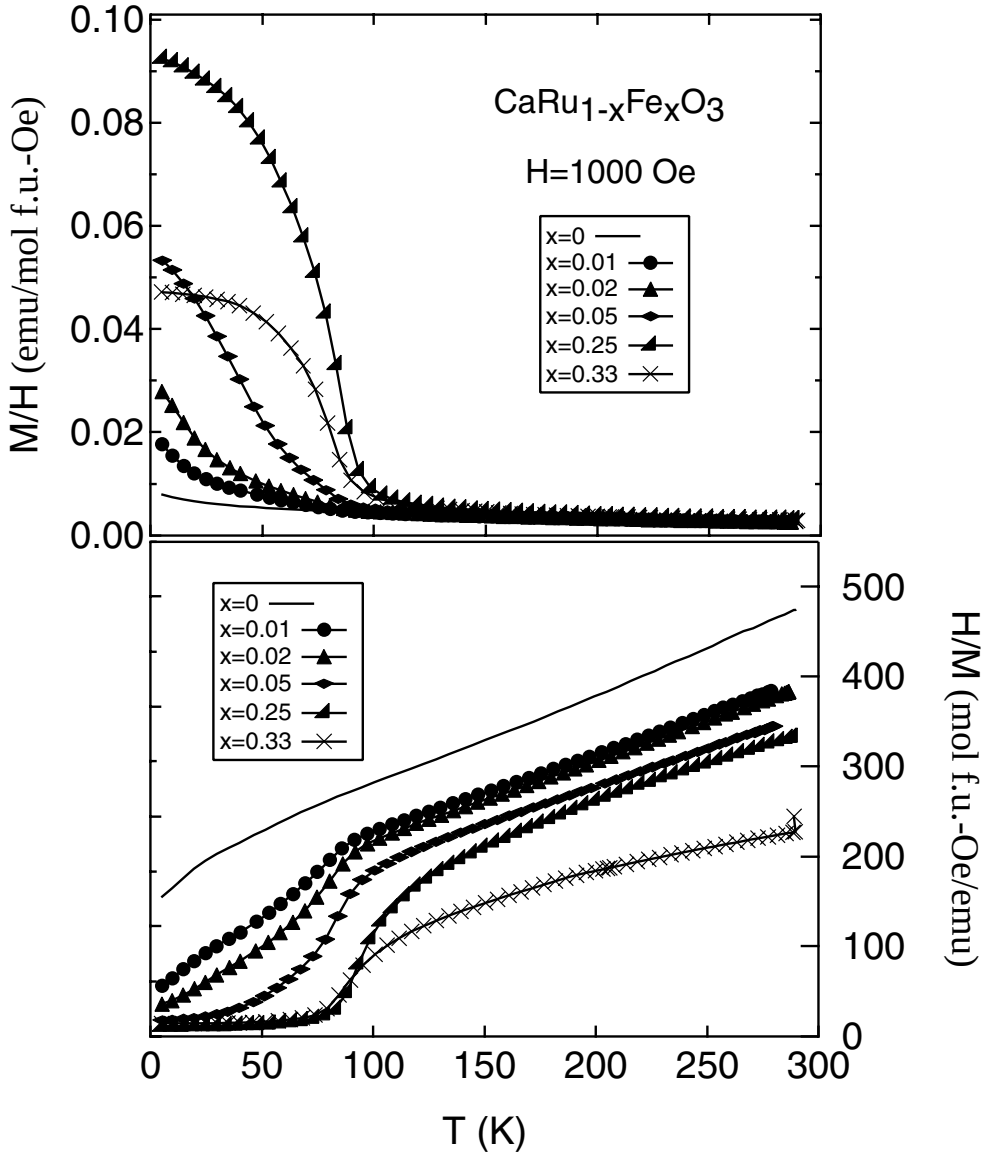

Figure 8. Temperature dependence of M/H (upper panel) and H/M (lower panel) measured at 1000 Oe on field cooling for $CaRu_{1-x}Fe_xO_3$ ($x = 0$, 0.01, 0.02, 0.05, 0.25 and 0.33).

very small or not observed. For those dopants, the M–H slopes are sometimes higher than that of $CaRuO_3$(5% Co^{2+}) and sometimes lower (5% V^{5+}, 5% Cu^{2+} and 25% Co^{2+}).

Among all the substitutions, Fe^{3+} and Mn^{4+} display the largest amounts of induced ferromagnetism in $CaRuO_3$. More detailed studies were therefore carried out on these two dopants. The magnetization of several $CaRu_{1-x}Fe_xO_3$ ($0 \leqslant x \leqslant 0.33$) samples was measured in the temperature range 5–300 K in an applied DC field of 1000 Oe on field cooling. The upper panel of figure 8 shows the temperature dependence of M/H for these samples. The highest doping level achieved for $CaRu_{1-x}Fe_xO_3$ is $x = 0.33$. At this doping level, the magnetization shows obvious saturation at low temperature indicating ferromagnetism. The magnetization at 5 K increases with x until $x = 0.25$ and then starts to decrease. The Curie temperature, T_C, which is estimated as the kink point, is about 100 K for all samples except $CaRuO_3$ itself.

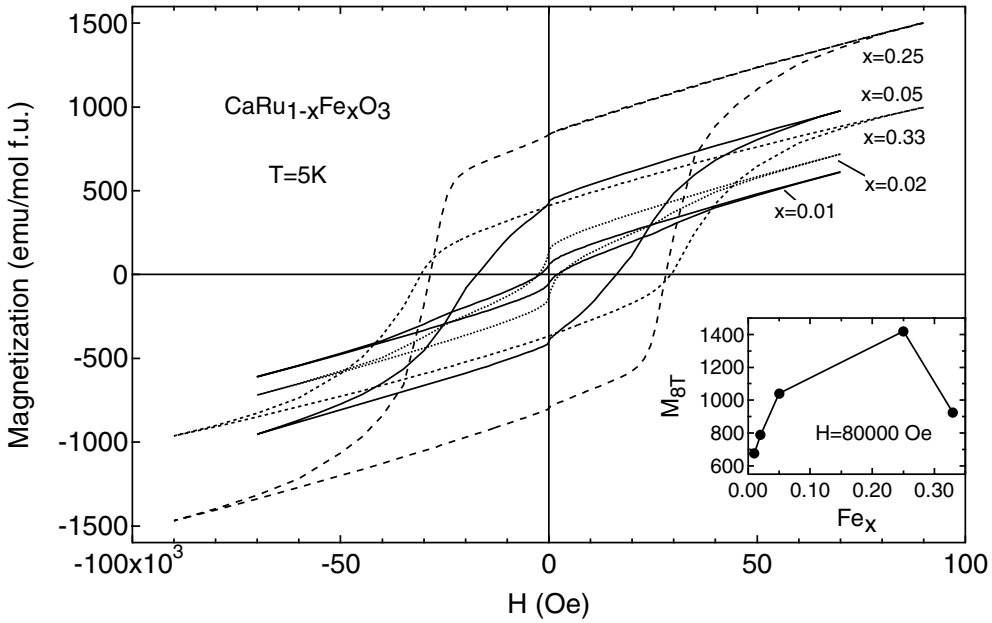

Figure 9. Magnetic hysteresis loops for $CaRu_{1-x}Fe_xO_3$ ($x = 0$, 0.01, 0.02, 0.05, 0.25 and 0.33) at 5 K.

This indicates that the temperature at which ferromagnetism turns on in $CaRu_{1-x}Fe_xO_3$ is of first order, independent of the Fe doping content. Studies on $CaRu_{1-x}Ti_xO_3$ reached the same conclusion, but with the critical temperature for $CaRu_{1-x}Ti_xO_3$ being 55 K [18]. The temperature dependence of H/M for $CaRu_{1-x}Fe_xO_3$ is shown in the lower panel of figure 8. H/M drops greatly when the temperature goes below 100 K. The Curie–Weiss temperature, θ_{CW}, however, remains negative for all samples even though the magnetization data show features of ferromagnetism. The magnetic hysteresis loops measured for $CaRu_{1-x}Fe_xO_3$ are shown in figure 9 and ferromagnetism is further confirmed. It is remarkable that as little as 1% Fe substitution creates a significant hysteresis loop. The coercive field increases with x. The remanent magnetization, however, increases until x equals 0.25 and then decreases as x approaches 0.33.

The same types of measurement were made for $CaRu_{1-x}Mn_xO_3$ ($0 \leqslant x \leqslant 0.75$). The upper panel of figure 10 shows the temperature dependence of the magnetization measured in low fields. Enhanced M/H is observed in the intermediate temperature range when Ru is substituted by Mn. The enhanced M/H is characteristic of the behaviour of ferromagnetic materials in low applied field. Unlike Fe doping, the magnetization at 5 K increases monotonically with increasing x. The Curie temperature, T_C, for $CaRu_{1-x}Mn_xO_3$ is about 195 K for all samples except $CaRuO_3$ itself. It is independent of the Mn doping content, as is the case for Ti and Fe doping. The lower panel of figure 10 shows the temperature dependence of H/M on $CaRu_{1-x}Mn_xO_3$. Of all the dopants studied, Mn is the only one that yields positive Curie–Weiss temperatures. Figure 11 shows the M–H loops for $CaRu_{1-x}Mn_xO_3$. The coercive field increases with x to 0.25 and then decreases with increasing x. The saturation magnetization, however, increases with increasing x, as is shown in the inset. $CaMnO_3$ itself is an antiferomagnet and the trend does not continue to higher Mn content [22].

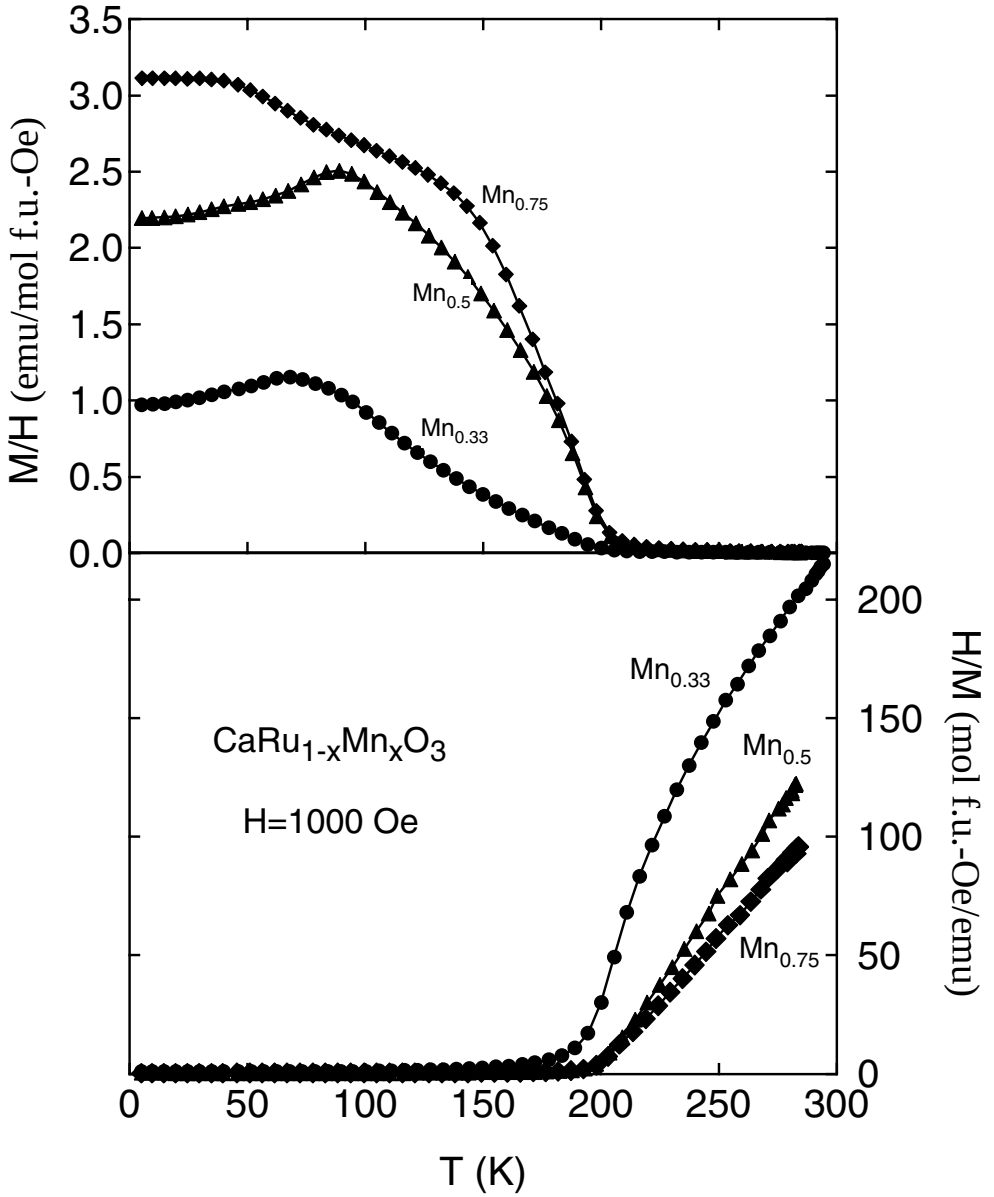

Figure 10. Temperature dependence of M/H (upper panel) and H/M (lower panel) measured at 1000 Oe on field cooling for $CaRu_{1-x}Mn_xO_3$ ($x = 0.33$, 0.5 and 0.75).

4. Summary and conclusion

The magnetic ground state of $CaRuO_3$ is problematic. The Ru-site doping experiments presented here and in other work support the proposal that it is best described as a nearly ferromagnetic metal. In the case of Ti^{4+} doping, the lack of a local moment and its valence matching Ru^{4+} means that disorder must be the dominant effect in inducing ferromagnetism [18]. The current study shows that $CaRuO_3$ can be made to display ferromagnetic behaviour

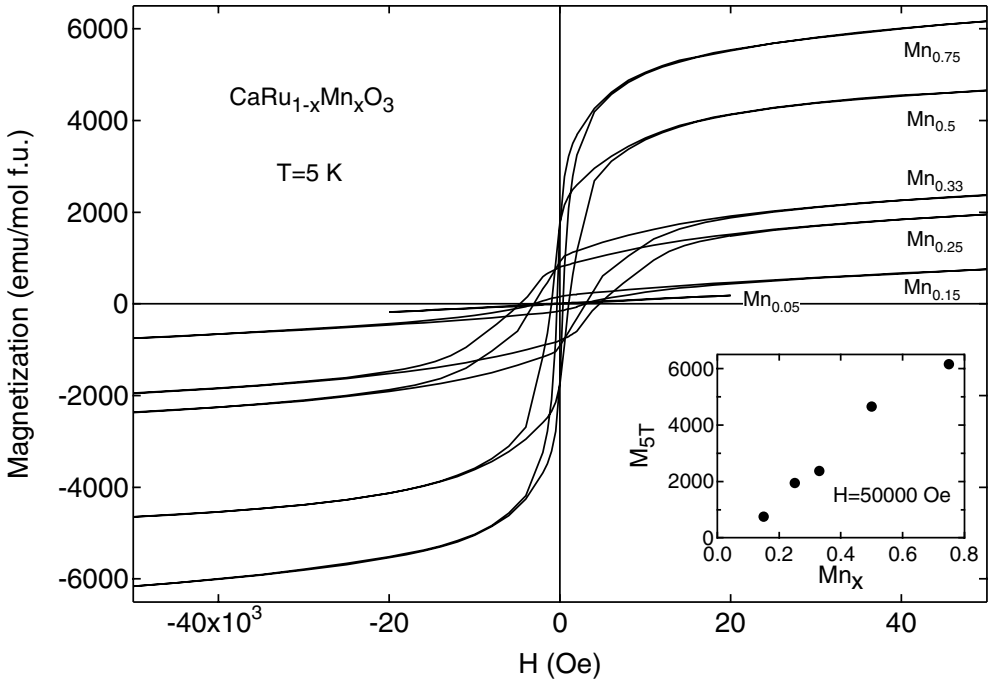

Figure 11. Magnetic hysteresis loops for $CaRu_{1-x}Mn_xO_3$ ($x = 0.05$, 0.15, 0.25, 0.33, 0.5 and 0.75) at 5 K.

by introducing very small amounts of many different substituents onto the Ru sites. The data are consistent with a picture in which $CaRuO_3$ itself is poised at a critical point between ferromagnetism and paramagnetism at low temperatures, a balance tipped in favour of the former by small amounts of impurities. The behaviour displayed by some of the systems is worthy of further consideration. We believe that the overall behaviour is consistent with an 'inhomogeneous' ferromagnetic system. In that case, small regions of ferromagnetism are induced by very small scale composition fluctuations within a single-phase solid solution. These ferromagnetic 'clusters' have an intrinsic T_C depending on the dopant ion and an increase in size or volume fraction with increasing dopant concentration maintains the same T_C.

Acknowledgment

This work was supported by the National Science Foundation Grant DMR-9725979.

References

[1] Callaghan A, Moeller C W and Ward R 1966 *Inorg. Chem.* **5** 1572
[2] Singh D J 1996 *J. Appl. Phys.* **79** 4818
[3] Maeno Y, Hashimoto H, Yoshida K, Nishizaki S, Fujita T, Bednorz J G and Lichtenberg F 1994 *Nature* **372** 532
[4] Mazin I I and Singh D J 1997 *Phys. Rev. Lett.* **79** 733
[5] Mazin I I and Singh D J 1999 *Phys. Rev. Lett.* **82** 4324
[6] Nakatsuji S, Ikeda S-I and Maeno Y 1997 *J. Phys. Soc. Japan* **66** 1868

[7] Cava R J, Zandbergen H W, Krajewski J J, Peck W F Jr, Batlogg B, Carter S, Flemming R M, Zhou O and Rupp L W Jr 1995 *J. Solid State Chem.* **116** 141
[8] Ikeda S-I and Maeno Y 1999 *Physica* B **261** 947
[9] Mazin I I and Singh D J 1998 *J. Phys. Chem. Solids* **59** 2185
[10] Fukunaga F and Tsuda N 1994 *J. Phys. Soc. Japan* **63** 3798
[11] Mazin I I and Singh D J 1997 *Phys. Rev.* B **56** 2556
[12] Santi G and Jarlborg T 1997 *J. Phys.: Condens. Matter* **9** 9563
[13] Cao G, McCall S, Shepard M and Crow J E 1997 *Phys. Rev.* B **56** 321
[14] Yoshimura K, Imai T, Kiyama T, Thurber K R, Hunt A W and Kosuge K 1999 *Phys. Rev. Lett.* **83** 4397
[15] Kiyama T, Yoshimura K, Kosuge K, Michor H and Hilscher G 1998 *J. Phys. Soc. Japan* **67** 307
[16] Kiyama T, Yoshimura K and Kosuge K 1999 *J. Phys. Soc. Japan* **68** 3372
[17] Mukuda H, Ishida K, Kitaoka Y, Asayama K, Kanno R and Takano M 1999 *Phys. Rev.* B **60** 12279
[18] He T and Cava R J 2001 *Phys. Rev.* B **63** 2403
[19] Klein L, Antognazza L, Geballe T H, Beasley M R and Kapitulnik A 1999 *Phys. Rev.* B **60** 1448
[20] Cao G, McCall S, Bolivar J, Shepard M, Freibert F, Henning P, Crow J E and Yuen T 1996 *Phys. Rev.* B **54** 15144
[21] Cao G, Freibert F and Crow J E 1997 *J. Appl. Phys.* **81** 3884
[22] Maignan A, Martin C, Hervieu M and Raveau B 2001 *Solid State Commun.* **117** 377
[23] Lightfoot P and Battle P D 1990 *J. Solid State Chem.* **89** 174
[24] Rijssenbeek J, Matl P, Ong N P and Cava R J 1998 *Phys. Rev.* B **58** 10315
[25] Frenzen S and Muller-Buschbaum H K 1995 *Z. Naturf.* b **50** 585
[26] McKenzie A P *et al* 1998 *Phys. Rev. Lett.* **80** 161